

The gamma-ray emitting microquasar LS I +61 303

M. Massi*, M. Ribó[†], J. M. Paredes**, S. T. Garrington[‡], M. Peracaula[§] and
J. Martí[¶]

*Max Planck Institut für Radioastronomie, Auf dem Hügel 69, D-53121 Bonn, Germany

[†]Service d'Astrophysique, CEA Saclay, Bât. 709, L'Orme des Merisiers, 91191 Gif-sur-Yvette,
Cedex, France

**Departament d'Astronomia i Meteorologia, Universitat de Barcelona, Av. Diagonal 647, 08028
Barcelona, Spain

[‡]Nuffield Radio Astronomy Laboratories, Jodrell Bank, Macclesfield, Cheshire SK11 9DL, UK

[§]Institut d'Informàtica i Aplicacions, Universitat de Girona, Campus de Montilivi s/n, 17071
Girona, Spain

[¶]Departamento de Física, Escuela Politécnica Superior, Univ. de Jaén, Virgen de la Cabeza 2,
23071 Jaén, Spain

Abstract. LS I +61 303 is one of the most studied X-ray binary systems because of its two peculiarities: On the one hand being the probable counterpart of the variable gamma ray source 2CG 135+01 [1, 2] and on the other hand being a periodic radio source [3]. The recent discovery of a radio emitting jet extending ca. 200 AU at both sides of a central core [4] in all evidence has shown the occurrence of accretion/ejection processes in this system. However, the radio outbursts do not occur at periastron passage, where the accretion is at its maximum, but several days later. In addition, when the gamma-ray emission of 2CG 135+01 is examined along the orbital phase of LS I +61 303 one sees that this emission seems to peak at periastron passage [5]. Here in detail we analyse the trend of the gamma-ray data versus orbital phase and discuss the delay between peaks at gamma-rays and in the radio band within the framework of a two-peak accretion/ejection model proposed by Taylor et al. [6] and further developed by Martí & Paredes [7].

THE BINARY STELLAR SYSTEM

The binary stellar system LS I +61 303 has an orbital period of 26.4960 days and a rather eccentric orbit ($e=0.7$) [8, 3, 7, 9, 10]. The visible companion is an early type, rapidly rotating B0Ve star [8, 10]. Be stars have a dense and slow ($<100 \text{ km s}^{-1}$) disk-like wind with a wind density distribution following a power law; a long monitoring of the H_α line emission has indicated that in the system LS I +61 303 are present variations in the mass loss with a period of about 4.6 years [11, 12, 13].

Through this dense, structured and variable envelope the compact object travels and accretes (see sketch in Fig. 1). It is still an open issue whether the compact object in this system is a neutron star or a black hole. Recent optical observations [10] give a mass function f in the range $0.003 < f < 0.027$. The maximum value of f for an inclination $i = 38^\circ$ and a mass of the Be star $M = 18M_\odot$ implies a mass of the compact object $M_X < 3.8M_\odot$; since the assumed upper limit for a stable neutron star is $3M_\odot$, the presence of a black hole in the system cannot be ruled out [5].

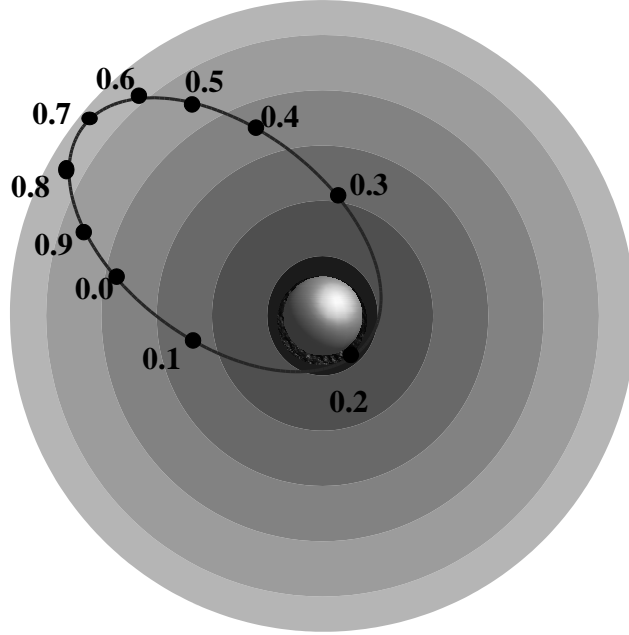


FIGURE 1. Sketch of the binary system LS I +61 303: Orbital phases of the compact object travelling through the wind of the Be companion (see text).

RADIO EMISSION

One of the most unusual aspects of the radio emission is that it exhibits two periodicities: a 26.4960 day periodic nonthermal outburst and a 4.6 years modulation of the outburst peak flux [3, 9]. The last period is clearly correlated with the mass loss of the Be star [11, 12, 13], whereas the shorter periodicity corresponds to the orbital period of the binary system [8, 10]. The variations of the Be equatorial disk influence, besides the outburst peak flux, the orbital phase where the outbursts occur and give rise to the observed broad distribution $\phi_{\text{radio-outbursts}}=0.45-0.95$ [14] where the phase is calculated for $t_0 = \text{JD } 2\,443\,366.775$ and $P = 26.4960$ days [9].

As shown in Fig. 1 the ϕ at periastron passage is 0.2 [10]. Therefore one of the fundamental questions concerning the periodic radio outbursts of LS I +61 303 has been: If the maximum accretion must occur where the density is highest, why are the radio outbursts delayed with respect to the periastron passage?

On the other hand the radio emission has been resolved with VLBI, EVN and MERLIN [15, 16, 4, 17]. The morphology of the radio emission in Fig. 2a (at $\phi=0.7$) is typical for a microquasar, i.e. jet-like, and constitutes the observational evidence of the occurrence of accretion/ejection processes in this system. Moreover, the morphology in Fig. 2a is S-shaped and quite similar to that of the precessing jet of SS 433 [18]. The receding jet is attenuated by Doppler de-boosting but still above the noise limit of the image. One day later (Fig. 2b) the precession suggested in the first MERLIN image becomes evident: a new feature is present oriented to the North-East at a position an-

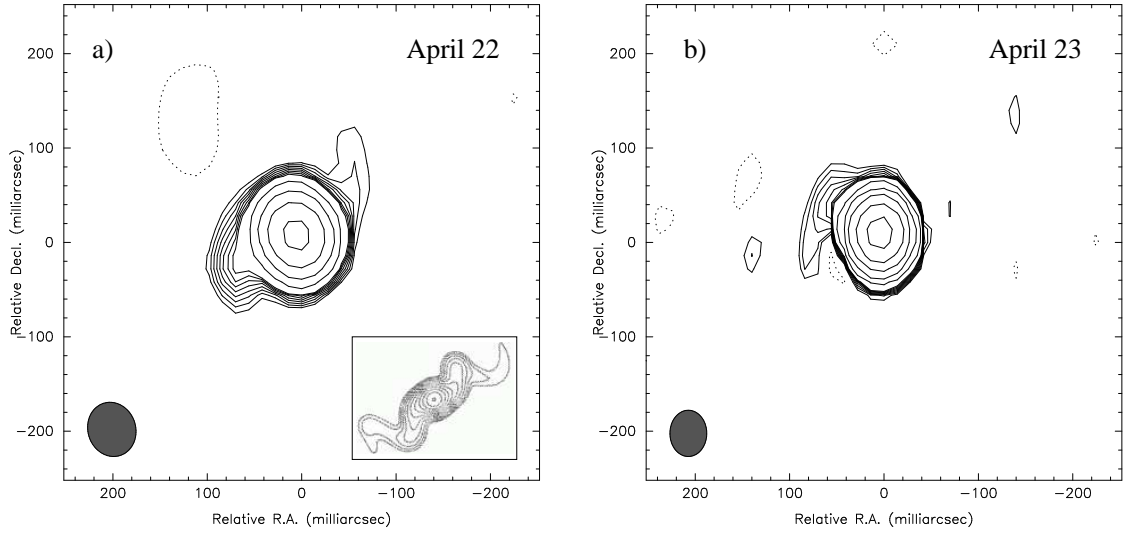


FIGURE 2. **a)** MERLIN image of LS I +61 303 at 5 GHz obtained on 2001 April 22. North is up and East is to the left. The synthesized beam has a size of 51×58 mas, with a PA of 17° . The contour levels are at $-3, 3, 4, 5, 6, 7, 8, 9, 10, 20, 40, 80,$ and 160σ , being $\sigma=0.14$ mJy beam $^{-1}$. The S-shaped morphology strongly recalls the precessing jet of SS 433, whose simulated radio emission (Fig. 6b in Hjellming & Johnston [18]) is given in the small box. **b)** Same as before but for the April 23 run. The synthesized beam has a size of 39×49 mas, with a PA of -10° . The contour levels are the same as those used in the April 22 image but up to 320σ , with $\sigma=0.12$ mJy beam $^{-1}$ [4].

gle (PA) of 67° ; the counter-jet is severely de-boosted. The Northwest-Southeast jet of Fig. 2a has a PA= 124° . Therefore a quite large rotation has occurred in only 24 hours.

GAMMA-RAY EMISSION

In 1978 Gregory and Taylor [1] reported about the discovery of a radio source (later on associated to LS I +61 303) within the 1σ error circle of the COS B γ -ray source 2CG 135+01. This association remained however controversial because of the presence of the quasar QSO 0241+622 within the relatively large COS B error box. The position of this gamma-ray source given as 2EG J0241+6119 in the Second EGRET Catalog is $l = 135^\circ.58, b = 1^\circ.13$; the radius of the 95% confidence error contour of about 13 arcminutes has finally ruled out the possible identification with QSO 0241+622, 64 arcminutes away. The position is, on the contrary compatible with LS I +61 303 only 8 arcminutes away [19]. In 1998 Tavani and collaborators establish the possibility of variability of 2CG 135+01 on timescales of days [2]. Massi [5] examines the EGRET data as a function of the orbital phase and notices the clustering of high flux around the ϕ interval 0.2–0.5 estimated to be the periastron passage.

Very recently Casares and collaborators [10] have finally confirmed periastron passage to be at $\phi=0.2$. Let us, therefore examine the plot of Fig. 3. The plot begins at the established periastron passage $\phi = 0.2$ and shows the follow-up of the EGRET gamma-ray emission along one full orbit. At epoch JD 2 450 334 (i.e. circles in the plot, with empty

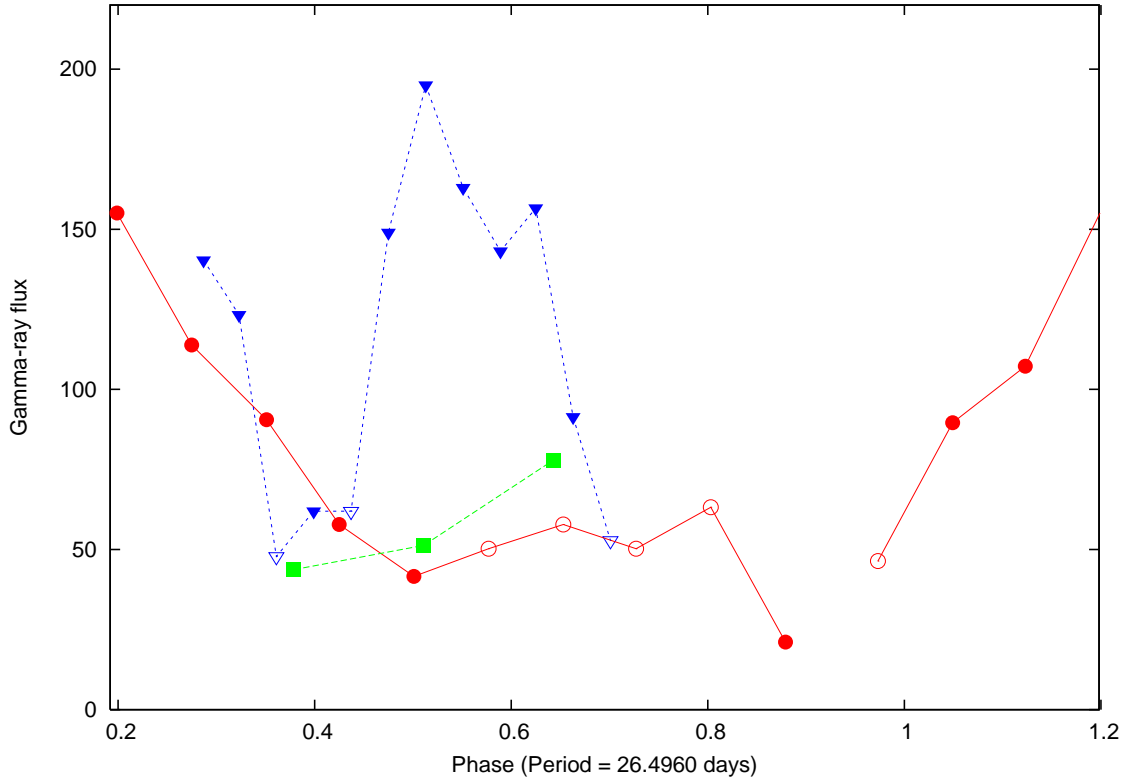


FIGURE 3. EGRET data vs. orbital phase (see text).

circles indicating upper limits) the orbit has been well sampled at all phases: A clear peak is centered at periastron passage 0.2 and 1.2. At a previous epoch (JD 2 449 045; triangles in the plot) the sampling is incomplete, still the data show an increase near periastron passage at $\phi \simeq 0.3$, and a peak at $\phi \simeq 0.5$. The 3 squares refer to a third epoch (JD 2 449 471).

THE TWO-PEAK ACCRETION/EJECTION MODEL

Taylor et al. [6] and Martí & Paredes [7] have modelled the properties of this system in terms of an accretion rate $\dot{M} \propto \frac{\rho_{\text{wind}}}{v_{\text{rel}}^3}$, (where ρ_{wind} is the density of the Be star wind and v_{rel} is the relative speed between the accretor and the wind) which develops two peaks for high eccentricities: the highest peak corresponds to the periastron passage (highest density), while the second peak occurs when the drop in the relative velocity v_{rel} compensates (because of the inverse cube dependence) the decrease in density. Martí & Paredes [7] have shown that both peaks are above the Eddington limit and therefore one expects that matter is ejected twice within the 26.5 days interval. During the first ejection, due to the proximity to the Be star, no radio emission but high energy emission is expected because of severe inverse Compton losses.

As a matter of fact whereas the few gamma-ray data available show high levels

TABLE 1. Luminosity (erg/s) [22]

$L_\gamma (> 100 \text{ MeV})$	L_X	L_{radio}
3.1×10^{35}	$(1-6) \times 10^{34}$	$(1-17) \times 10^{31}$

of gamma-ray emission around periastron passage (previous section), radio outbursts were indeed never observed at periastron passage in more than 20 years of radio flux measurements. Moreover, Bosch-Ramon and Paredes [20] have proposed a numerical model based on inverse Compton scattering where the relativistic electrons in the jet are exposed to stellar photons (external Compton) as well as to synchrotron photons (synchrotron self Compton). This model considers accretion variations along the orbit and predicts indeed a gamma-ray peak at periastron passage where the accretion is higher.

At the second accretion peak the compact object is enough far away from the Be star, so that the inverse Compton losses are small and electrons can propagate out of the orbital plane. Then an expanding double radio source should be observed, what in fact has been observed (Fig. 1) by MERLIN at orbital phase 0.7 (apoastron). Interesting in this respect is the gamma-ray peak at $\phi \simeq 0.5$ that could originate from a second ejection which occurred still close enough to the Be star.

CONCLUSIONS

It is clear that new gamma-ray observations are desirable to confirm the periodical gamma-ray flares at periastron passage predicted by the model. For a second ejection still close enough to the Be star in order to generate a second gamma-ray flare, joint radio observations would allow to determine important physical parameters. The radio and gamma-ray peaks are expected to be delayed: When the electrons start to produce synchrotron emission in the radio band, this emission is absorbed by the thermal electrons of the Be wind. Such a delay strongly depends on the distance from the Be star.

In ejections distant enough from the Be star it could be verified if also disk photons are upscattered by the relativistic electrons and contribute to the gamma-ray emission [21], such a contribution would finally explain why LS I +61 303 is subluminescent in the X-ray range (see Table 1, adapted from [22]).

Moreover, on the basis of the precession shown in Fig. 2, we suggest that the fast precession bringing the jet intermittently closer and farther to the line of sight should produce noticeable variable γ -ray emission. In fact, the amplification due to the Doppler factor for Compton scattering of stellar photons by the relativistic electrons of the jet is even higher than that for synchrotron emission [21, 4]. In conclusion LS I +61 303 becomes the ideal laboratory to test the recently proposed model for microblazars with INTEGRAL and MERLIN observations now and by AGILE and GLAST in the future.

ACKNOWLEDGMENTS

MERLIN is operated as a National Facility by the University of Manchester at Jodrell Bank Observatory on behalf of the UK Particle Physics & Astronomy Research Council. M. R., J. M. P. and J. M. acknowledge partial support by DGI of the Ministerio de Ciencia y Tecnología (Spain) under grant AYA2001-3092, as well as partial support by the European Regional Development Fund (ERDF/FEDER). M. R. acknowledges support by a Marie Curie Fellowship of the European Community programme Improving Human Potential under contract number HPMF-CT-2002-02053. M. P. acknowledges financial support by the program ‘Ramón y Cajal’ of the Ministerio de Ciencia y Tecnología (Spain). J. M. has been aided in this work by an Henri Chrétien International Research Grant administered by the American Astronomical Society, and has been partially supported by the Plan Andaluz de Investigación of the Junta de Andalucía (ref. FQM322).

REFERENCES

1. Gregory, P.C., & Taylor, A.R., *Nature*, **272**, 704–706 (1978).
2. Tavani, M., Kniffen, D., Mattox, J.R., Paredes, J.M., & Foster, R.S., *ApJ*, **497**, L89–L91 (1998).
3. Taylor, A.R., & Gregory, P.C., *ApJ*, **255**, 210–216 (1982).
4. Massi, M., Ribó, M., Paredes, J.M., Garrington, S.T., Peracaula, M., & Martí, J., *A&A*, **414**, L1–L4 (2004).
5. Massi, M., *A&A*, **422**, 267–270 (2004).
6. Taylor, A.R., Kenny, H.T., Spencer, R.E., & Tzioumis, A., *ApJ*, **395**, 268–274 (1992).
7. Martí, J., & Paredes, J.M., *A&A*, **298**, 151–158 (1995).
8. Hutchings, J.B., & Crampton, D., *PASP*, **93**, 486–489 (1981).
9. Gregory, P.C., *ApJ*, **575**, 427–434 (2002).
10. Casares, J., Ribas, I., Paredes, J.M., Martí, J., & Allende Prieto, C., *MNRAS*, submitted (2004).
11. Zamanov, R.K., Martí, J., Paredes, J.M., Fabregat, J., Ribó, M., & Tarasov, A.E., *A&A*, **351**, 543–550 (1999).
12. Zamanov, R.K., & Martí, J., *A&A*, **358**, L55–L58 (2000).
13. Gregory, P.C., & Neish, C., *ApJ*, **580**, 1133–1148 (2002).
14. Paredes, J.M., Estalella, R. & Rius, A., *A&A*, **232**, 377–380 (1990).
15. Massi, M., Paredes, J.M., Estalella, R., & Felli, M., *A&A*, **269**, 249–254 (1993).
16. Massi, M., Ribó, M., Paredes, J.M., Peracaula, M., & Estalella, R., *A&A*, **376**, 217–223 (2001).
17. Paredes, J.M., Massi, M., Estalella, R., & Peracaula, M., *A&A*, **335**, 539–544 (1998).
18. Hjellming, R.M., & Johnston, K.J., *ApJ*, **328**, 600–609 (1988).
19. Kniffen, D.A., Alberts, W.C.K., Bertsch, D.L., Dingus, B.L., Esposito, J.A., et al., *ApJ*, **486**, 126–131 (1997).
20. Bosch-Ramon, V., & Paredes, J.M., *A&A*, **425**, 1069–1074 (2004).
21. Kaufman Bernadó, M.M., Romero, G.E., & Mirabel, I.F., *A&A*, **385**, L10–L13 (2002).
22. Combi, J.A., Ribó, M., Mirabel, I.F., & Sugizaki, M., *A&A*, **422**, 1031–1037 (2004).